THE JOURNAL OF PHYSICAL CHEMISTRY C

Article

pubs.acs.org/JPCC

Beyond Graphitic Carbon Nitride: Nitrogen-Rich Penta-CN_2 Sheet

Shunhong Zhang,[†] Jian Zhou,[‡] Qian Wang,*[,†,‡] and Puru Jena[‡]

[†]Center for Applied Physics and Technology (CAPT), Key Laboratory of High Energy Density Physics Simulation, Peking University, Beijing 100871, China

[‡]Department of Physics, Virginia Commonwealth University, Richmond, Virginia 23284, United States

Supporting Information

ABSTRACT: Using first-principles calculations combined with *ab initio* molecular dynamics and tight binding model, we predict the existence of a kinetically stable two-dimensional (2D) penta-CN_2 sheet, which is isostructural to the recently discovered penta-graphene. The concentration of N in this new carbon nitride sheet exceeds the maximum N content, namely 21.66%, that has been achieved experimentally in honeycomb geometry. It even exceeds the N content found recently in hole-doped carbon nitride $C_{0.5}N_{0.5}$ as well as in porous graphitic C_3N_4. The penta-CN_2 sheet contains N−N single bonds with an energy density of 4.41 kJ/g, higher than that predicted recently in nitrogen-rich B−N compound. Remarkably, penta-CN_2 has an in-plane axial Young's modulus of 319 N/m, even stiffer than the *h*-BN monolayer. The electronic band structure of penta-CN_2 exhibits an interesting double degeneracy at the first Brillouin zone edges which is protected by the nonsymmorphic symmetry and can be found in other isostructural chemical analogues. The band gap of penta-CN_2 calculated using HSE06 functional is 6.53 eV, suggesting its insulating nature. The prediction of a stable penta-CN_2 implies that puckering might be more effective than porosity in holding nitrogen in 2D carbon nitrides. This sheds new light on how to design nitrogen-rich C−N compounds beyond N-doped graphene.

INTRODUCTION

Carbon nitride belongs to a large family of inorganic materials that epitomizes varying stoichiometry, rich chemistry, and exceptional properties. Bulk β-C_3N_4[1,2] and layered graphitic-C_3N_4[3] are the two most well-known carbon nitride polymorphs. Besides these, many other carbon nitride materials have also been synthesized or predicted, both in bulk[4−7] and in nanostructured forms.[8−16] The C−N compounds have broad applications in mechanics,[4] optoelectronics,[17] magnetics,[9,16] and catalysis.[13,18] In addition, nitrogen-rich nitride materials may have potential application as high energy density materials (HEDM). Hence their design and synthesis are hotly pursued fields of research in materials science.

To facilitate the application of nitrogen-rich materials as HEDM, two challenges must be addressed. The first one is to increase the nitrogen content. Many efforts have been made to find ways to increase the uptake of nitrogen in carbon nitride materials.[11,19−21] However, these studies mainly focused on planar graphitic structures derived from nitrogen-doped graphene. It was demonstrated[19] that the largest achievable N doping concentration in graphitic structures is 33.3%−37.5%. When the nitrogen content increases, strong interactions between the neighboring N atoms leads to the formation of diatomic molecules,[21] consequently, destroying the honeycomb structure.[10,11,19] Raising the nitrogen content beyond C_3N_4 has been a desired goal.

The second challenge in HEDM is to have N−N single bonds in nitrogen-rich materials so that they can release substantial amount of energy when the structure decomposes and forms triply bonded N_2 molecules. To this end several strategies have been suggested. Direct compression of gaseous nitrogen is one of the most widely adopted methods which has led to the discovery of the well-known cubic-gauche phase[22] in which all nitrogen atoms form single bonds with each other, forming a polymeric phase. Another effective approach is to stabilize singly bonded polymeric nitrogen atoms by confining them in some host structures such as carbon nanotubes[23] or graphene matrix.[24] Chemists have also found that metal azides[25,26] may serve as HEDM as they contain singly bonded N_3^- moieties. Generally, the former two strategies require external constraints and the polymeric nitrogen structures may not be stable at ambient conditions. In metal azides, the existence of heavy metal atoms decrease the energy density. Thus, developing new light-element based covalently bonded HEDMs that can be metastable at ambient condition is of great significance.

Bearing the above two challenges in mind, we tried to go beyond graphitic carbon nitride to design new nitrogen-rich 2D carbon nitride materials. Unlike previous works that focused on nitrogen-doped graphene, we started searching for new C−N compounds that may mimic the structure of the recently predicted all-pentagon carbon allotrope, penta-graphene.[27] The novel mechanical and electronic properties of penta-graphene have drawn considerable attention, and some of its isostructural

Received: December 22, 2015
Revised: January 25, 2016
Published: January 28, 2016

DOI: 10.1021/acs.jpcc.5b12510
J. Phys. Chem. C 2016, 120, 3993−3998

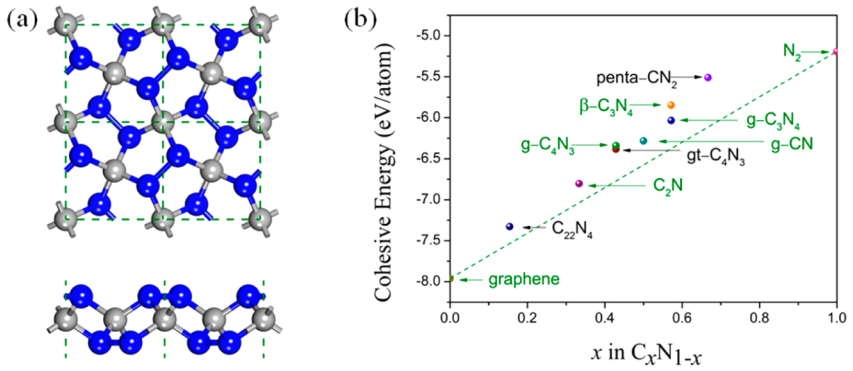

Figure 1. (a) Top (upper panel) and side (lower panel) views of optimized structure of penta-CN_2. Gray and blue spheres represent carbon and nitrogen atoms, respectively. The green dash lines mark the unit cell. (b) Cohesive energy of some C_xN_{1-x} compounds. The green dash line connecting the chemical potential of C (graphene) and N (N_2 molecule) is used to gauge the formation energy. The formation energy is positive (negative) above (below) the line. Structures marked with green texts have been experimentally synthesized. For structural details, one can refer to pertinent papers (β-C_3N_4,[2] g-CN,[14] g-C_4N_3,[9] gt-C_4N_3,[15] C_2N,[10] and $C_{22}N_4$[18]).

compounds such as penta-SiC_2[28] and penta-B_2C[29] have been proposed. Even in confined 2D ice system the water molecules were found to form a penta-graphene-like Cairo-pentagon pattern.[30] The experimentally realized HEDM, silver azide (AgN_3), has a layered structure, and in each layer, the 4-coordinated Ag atoms link to the azide moieties, forming an atomic Cairo-pentagon tiling-like structure.[25] These findings inspire us to further explore if there exists any other compound composed of light-elements that can adopt such an exotic atomic configuration.

In this paper, we propose a 2D all-pentagon carbon-nitride sheet with a chemical formula, CN_2. Using first-principles calculations we show that this new structure, termed as penta-CN_2, is thermally and dynamically stable. Penta-CN_2 has a large puckering height which helps it to accommodate more nitrogen atoms compared to planar graphitic structures. The strong interatomic bonding leads to a high in-plane elastic modulus that is even larger than that of monolayer *h*-BN. Equally important, the N_2 units in this compound form single bonds, enabling this material to have potential as a 2D HEDM. In addition, a chemically analogous penta-SiN_2 sheet is also investigated and its properties are compared with penta-CN_2. By carefully inspecting the band structure of penta-CN_2, penta-SiN_2, along with previously studied penta-graphene, petna-B_2C, and penta-SiC_2, we identify a universal band degeneracy which is protected by the structural symmetry and can be understood using a simple tight-binding model.

COMPUTATIONAL METHODS

We use Vienna *ab initio* simulation package (VASP)[31] to perform density functional theory (DFT) based first-principles calculations. The projector augmented wave (PAW) method[32] is used to treat the core electrons. The wave functions of valence electrons ($2s^22p^2$ for C, $3s^23p^2$ for Si and $2s^22p^3$ for N) are expanded using plane-wave basis sets with an energy cutoff of 500 eV. We use the PBE functional[33] for primary electronic structure calculations and HSE06[34,35] hybrid functional for the band gap. The 2D structures are simulated using periodic boundary conditions and by adding a vacuum space of 15 Å along the *z* direction to avoid interactions between the different nearest neighboring layers. The first Brillouin zone is sampled by a (13 × 13) K point grid using the Monkhorst−Pack[36] scheme. Conjugated gradient algorithm is adopted to relax the structures and the convergence criteria for total energy and force components are set to be 10^{-4} eV and 10^{-3} eV/Å, respectively. Phonon spectra are calculated by using density functional perturbation theory (DFPT)[37] as implemented in the Quantum ESPRESSO[38] code. The Martins−Troullier norm-conserving pseudopotential[39] is used to treat the core electrons while valence electron wave functions are expanded using plane waves with an energy cutoff of 60 Ry. Raman activity and infrared intensity are calculated using the second-order response method.[40]

RESULTS AND DISCUSSION

The optimized structure of penta-CN_2 is shown in Figure 1a. This nitrogen-rich 2D compound has a tetragonal lattice with a lattice parameter a = 3.31 Å, and is crystallographically subject to the $P\bar{4}2_1m$ layer group (No. 58). The relaxed structure of penta-CN_2 is composed of three atomic layers with C atoms in the middle and N atoms on the top and bottom, similar to that of penta-graphene. In this structure, all C atoms are sp^3 hybridized. The "thickness" of this sheet defined as the vertical coordinates difference between the nitrogen atoms in the top and bottom layers is 1.52 Å, which is larger than that of penta-graphene (1.20 Å) and its other covalent chemical analogues (B_2C, 1.08 Å;[29] SiC_2, 1.33 Å[28]). We note that previous studies attempted to find dynamically stable planar CN[11] or CN_2[13] allotropes via global structure search but failed. Here the highly puckered structure of penta-CN_2 implies that buckling may be essential during the formation and stabilization of nitrogen-rich 2D carbon nitride compounds. Indeed, such puckering is commonly seen in 2D structures with electron-rich nitrogen-group atoms, such as the honeycomb structure of phosphorene.[41] We also find that the C and N atoms are singly bonded with a bond length of 1.47 Å. Each C atom transfers about 1.2 electrons to N atoms according to our Bader's charge analysis,[42] implying a significant polarizability of the C−N covalent bonds. Compared with previously proposed N chains encapsulated in carbon nanotubes,[23] the nitrogen atoms in penta-CN_2 receive much more charge, indicating a stronger interaction. The reason that penta-CN_2 differs from previously identified 2D C−N compound is because in this structure N−N dimers exist. Unlike the recently identified TiN_{12} cluster[43] where N_2 dimers binds to the Ti atom quasi-molecularly, the N−N bond length in this compound reaches 1.45 Å, which explicitly shows a single bond character. Although N−N single bond has been observed in some high pressure polymeric phase of gas

DOI: 10.1021/acs.jpcc.5b12510
J. Phys. Chem. C 2016, 120, 3993−3998

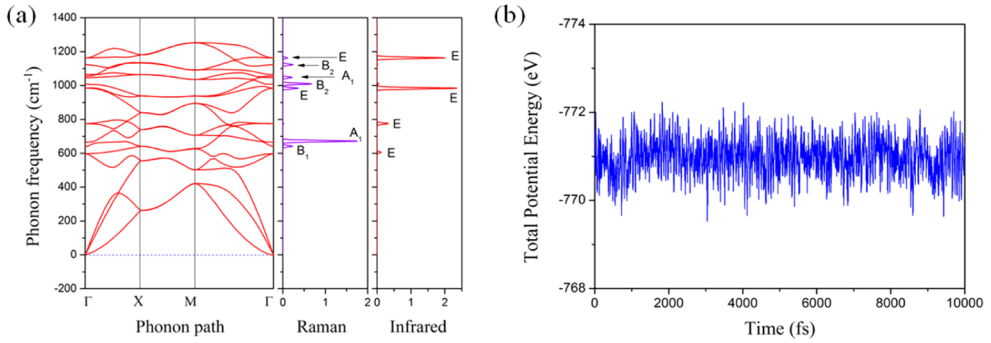

Figure 2. (a) Phonon spectra of penta-CN_2, as well as the Raman and infrared intensity (in arbitrary units) of the zone center vibrational modes. A uniform Gaussian broadening of 10 cm^{-1} is used in the plot of Raman and infrared spectra. High symmetric q point paths are Γ (0, 0), X (1/2, 0), and M (1/2, 1/2). (b) Fluctuation of potential energy of penta-CN_2 (4 × 4 supercell) during a NVT AIMD simulation at 300 K.

molecules,[22] it is rarely seen in covalent crystals at ambient pressure. Because of the remarkable difference in bond energies between single (160 kJ/mol) and triple (954 kJ/mol) nitrogen bonds,[44] the emergence of singly bonded N−N unit can facilitate storage of a large amount of energy in this material. When decomposed, the formation of nitrogen molecules may lead to release of energy and the material is thus a good candidate for HEDM. To gauge how much energy can be released when the compound decomposes, we calculated the cohesive energy of some known C_xN_{1-x} compounds and defined the formation energy[19,45] as

$$E_f(C_xN_{1-x}) = E_{coh}(C_xN_{1-x}) - x\mu_C - (1-x)\mu_N$$

Here E_{coh} (C_xN_{1-x}) is the cohesive energy of the C_xN_{1-x} compound (in eV per atom). The chemical potential of C and N (μ_C and μ_N) are taken from the cohesive energy of graphene and molecular N_2, respectively. The calculated formation energy of penta-CN_2 reaches 0.61 eV, equivalent to an energy density of ∼4.41 kJ/g. This value is larger than that of the recently predicted metastable nitrogen-rich B_3N_5 compound (∼3.44 kJ/g)[46] formed under high pressure. Both the high nitrogen content and the emergence of N−N single bonds, as stated above, are critical to the high energy density of penta-CN_2. Thus, this compound can be utilized as a potential HEDM.

The positive formation energy is also an indication of metastability of penta-CN_2. In fact, due to the extraordinarily strong triple bond in nitrogen molecule, most C−N compounds, including previously studied graphene-like C−N alloys,[8,19] have positive formation energy, as shown in Figure 1b. However, the metastable nitrogen-rich C_3N_4 polymorphs have been experimentally realized both in bulk and layered forms. We therefore believe that the synthesis of penta-CN_2 sheet should also be thermodynamically possible. Indeed, we note that a bulk CN_2 phase suggested in a prior work[7] can be considered as a structure of stacked penta-CN_2 layers. This bulk tetragonal phase, with remarkable thermodynamic stability, may serve as a precursor to realize monolayer penta-CN_2. In fact, experimentalists have successfully synthesized a nitrogen-rich structure with a N:C ratio of 1.87,[47] which may give us the hope of further raising the ratio up to 2 as in the proposed penta-CN_2 sheet.

To verify if penta-CN_2 belongs to a local minimum on the potential energy surface, we have calculated its phonon spectra. The absence of imaginary mode in the whole 2D reciprocal space indicates that this nanosheet is dynamically stable (Figure 2a). To guide future characterization of penta-CN_2 in experiments, we calculated the Raman and infrared spectra of the zone center phonon modes (Figure 2a). The zone center vibrational modes have D_{2d} symmetry and the corresponding irreducible representation can be expressed as

$$\Gamma(\text{penta-}CN_2) = 5E(I+R) \oplus 2B_1(R) \oplus 3B_2(I+R) \oplus 2A_1(R) \oplus A_2$$

where "I" and "R" represent the infrared and Raman activity of the mode, respectively. The details of all vibrational modes are given in Figure S1. The A_1 mode (671.7 cm^{-1}) corresponding to the vibration of N_2 dimers has the strongest Raman activity. We see that the large phonon gap exhibited in penta-graphene[27] disappears in the phonon spectra of penta-CN_2 because all the interatomic bonds in this compound are single bonds while in penta-graphene C═C double bonds exist.

To further check the thermal stability of penta-CN_2 at finite temperature, *ab initio* molecular dynamics (AIMD) simulations are performed in a (4 × 4) supercell. After heating at 300 K for 10 ps with a time step of 1 femtosecond (*fs*), the structure does not suffer significant distortion or transformation. The total potential energy only fluctuates around a constant magnitude (Figure 2b). We also perform similar simulation using a $4(\sqrt{2} \times \sqrt{2})$ R45° supercell, and found no structure reconstruction either. These simulations indicate that the penta-CN_2 is thermally stable at room temperature.

Using the finite distortion method,[27] we calculated the linear elastic constants of penta-CN_2. The 2D linear elastic constants are found to be $C_{11} = C_{22} = 319$ N/m, $C_{12} = 22$ N/m. These comply with the Born criteria and confirm that penta-CN_2 is mechanically stable. The in-plane axial Young modulus is $E = (C_{11}^2 - C_{12}^2)/C_{11} = 318.5$ N/m, which is close to that of graphene (345 N/m[48]). Penta-CN_2 is stiffer than previously studied porous graphitic carbon nitrides sheets,[15] and is even stiffer than *h*-BN monolayer (271 N/m[49]). The unexpected high in-plane stiffness of penta-CN_2 can be viewed as a result of strong interatomic bonding.[50] This can be further confirmed by calculating the in-plane sound velocity of the compound. At the long wavelength limit, by fitting the longitudinal acoustic modes near the Γ point, we obtain the speed of sound along the axial lattice direction to be 15.4 km/s, much higher than that of other 2D materials such as phosphorene.[41]

The electronic band structure of penta-CN_2 is calculated and plotted in Figure 3a. The valence band maximum (VBM) is on the M−Γ path while the conduction band minimum (CBM) is located on the Γ−X path. An indirect band gap of 4.83 eV is

DOI: 10.1021/acs.jpcc.5b12510
J. Phys. Chem. C 2016, 120, 3993−3998

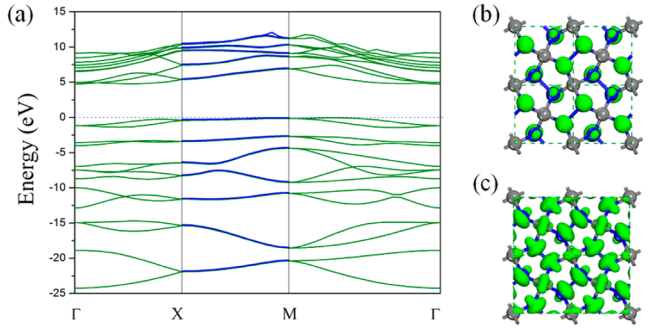

Figure 3. (a) Electronic band structure of penta-CN_2, and charge density distribution of (b) the valence band and (c) the conduction band. The value of isosurface in parts b and c is 0.1 e/Å.[3] Blue lines in part a indicate the doubly degenerate bands along the X−M path.

predicted using the PBE functional. By using a more accurate hybrid functional HSE06, we verify that the band dispersion profiles remain the same (Figure S2), but the band gap value is increased to 6.53 eV. The calculated band-decomposed charge density distribution suggests that the two highest occupied bands are dominated by the electron lone pairs on the N atoms, while the two lowest unoccupied bands are contributed by the antibonding states of both C−N and N−N bonds.

It is interesting that the energy bands of penta-CN_2 are all doubly degenerate along the X → M path, as shown by the blue lines in Figure 3. In the proximity of the X and M points the dispersion of the two highest occupied bands has a nearly linear k dependence, forming 2D energy bands with Dirac points and nodal lines. Electrons with such band dispersion behave like relativistic electrons, rather than the common nonrelativistic electrons described by the Schrödinger's equation. We argue that the nonsymmorphic layer group $P\bar{4}2_1m$, which composes screw axes operations $\left\{C_{2\hat{x}}\middle|\frac{1}{2}\frac{1}{2}\right\}$ and $\left\{C_{2\hat{y}}\middle|\frac{1}{2}\frac{1}{2}\right\}$ is responsible for such degeneracy. According to Young and Kane,[51] in the band dispersion of a 2D structure with nonsymmorphic symmetry $\{g|\mathbf{t}\}$ the bands at the invariant points in the Brillouin zone that satisfy $g\mathbf{k} = \mathbf{k}$, are topologically protected to "stick together". In the case of penta-CN_2 which is subjected to P-42_1m group, such invariant points are located at the boundary of the first Brillouin zone, namely, along the X → M path. In order to prove this symmetry protected band degeneracy, we apply a simple tight binding model to reproduce the band dispersion (spin−orbit coupling is not included due to negligible values for C and N atoms)

$$\hat{H} = \sum_{\langle i,j\rangle,\sigma}^{i\in C, j\in N_\sigma} t_\sigma(\hat{c}_i^\dagger \hat{c}_j + \text{h.c.}) + t\sum_{\langle i,j\rangle}^{i,j\in N_\sigma}(\hat{c}_i^\dagger \hat{c}_j + \text{h.c.}) + \sum_{\sigma,i\in N_\sigma} U_\sigma(\hat{c}_i^\dagger \hat{c}_i + \text{h.c.})$$

where $c^\dagger$ and c are electron creation and annihilation operators, respectively. $\sigma = \uparrow$ and $\downarrow$ denote the upper and lower sublattices of N layers, respectively. t and U are hopping integral and on-site Hubbard term, respectively. The first term in the Hamiltonian is the interlayer hopping term between the C and N atoms, the second term is the intralayer N−N hopping within the N layers, and the third term denotes the on-site energy in the upper (lower) N layer. By diagonalizing the Hamiltonian, we obtain the band dispersion along the high symmetry k-path. When $t_\uparrow = t_\downarrow$ (= 0.4t) and $U_\uparrow = U_\downarrow$, the screw axes symmetry operations $\left\{C_{2\hat{x}}\middle|\frac{1}{2}\frac{1}{2}\right\}$ and $\left\{C_{2\hat{y}}\middle|\frac{1}{2}\frac{1}{2}\right\}$ hold, we can see that each two bands along the X → M path stick together (Figure 4a). However, if we tune the hopping integral

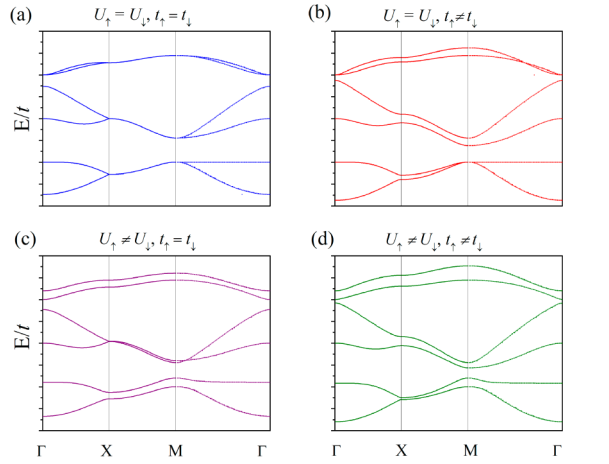

Figure 4. Tight binding band dispersion of the penta-CN_2 model with different setups: (a) $t_\uparrow = t_\downarrow$ = 0.4t and $U_\uparrow = U_\downarrow = 0$, (b) $t_\uparrow$ = 0.5t, $t_\downarrow$ = 0.4t, and $U_\uparrow = U_\downarrow = 0$, (c) $t_\uparrow = t_\downarrow$ = 0.4t, $U_\uparrow$ = 0.2t, and $U_\downarrow = 0$, and (d) $t_\uparrow$ = 0.5t, $t_\downarrow$ = 0.4t, $U_\uparrow$ = 0.2t, and $U_\downarrow = 0$.

to $t_\uparrow$ = 0.5t and keep $t_\downarrow$ = 0.4t (Figure 4b), the screw axes symmetry is violated and the band degeneracy is clearly lifted. Similar band splitting can be observed when $U_\uparrow \neq U_\downarrow$ while keeping $t_\uparrow = t_\downarrow$ (Figure 4c), or when both $U_\uparrow \neq U_\downarrow$ and $t_\uparrow \neq t_\downarrow$ (Figure 4d). These results agree with that of the generalized theoretical analysis and thus demonstrate that the Dirac points and nodal lines degeneracy in bands along the X → M are topologically protected by nonsymmorphic symmetry. We expect that penta-CN_2 can behave as a 2D Dirac semimetal when it is slightly p-doped. In fact, we examine the band structures of previously studied penta-graphene,[27] penta-SiC_2,[28] and penta-B_2C (which have the same nonsymmorphic symmetry operations),[29] and find that all their dispersions exhibit similar feature, confirming that the universal band degeneracy in these compounds is intimately related to the structural symmetry.

It would be interesting to see how the geometry and electronic band structure change when the penta-CN_2 monolayers are stacked. Herein three stacking patterns are studied. We found that the energetically most favorable pattern is AA stacking (Figure S3a). The patterns in Figure S3, parts b and c are 0.10 and 0.11 eV per unit cell higher in energy than that of the AA stacking configuration, respectively. The optimized interlayer distance is 4.15, 4.78, and 4.74 Å, respectively for the three patterns when the van der Waals interaction is taken into account via adding the Grimme's potential.[52] However, even in the AA stacking, the interplay between the two layers is rather weak, which can be further manifested by calculating the band structures: from Figure S4, we can see that the bands structures of bilayer penta-CN_2 inherits the main feature of the band structure of monolayer. The calculated band gaps are respectively 4.69, 4.50, and 4.60 eV when calculated using the PBE functional, all the values close to that of the monolayer.

For comparison, we have also systematically studied the chemically analogous penta-SiN_2 by replacing all C atoms in penta-CN_2 with Si atoms. The main results are summarized in

DOI: 10.1021/acs.jpcc.5b12510
J. Phys. Chem. C 2016, 120, 3993−3998

Table 1. Summary of Structural Parameters and Basic Properties of Penta-CN_2 and Penta-SiN_2

	penta-CN_2	penta-SiN_2
lattice constant (Å)	3.31	4.04
thickness (Å)	1.52	1.41
N−N bond length (Å)	1.47	1.47
charge transfer (e/nitrogen)	0.6	1.5
formation energy (eV/atom)	0.61	−0.14
band gap (eV)	PBE: 4.83	PBE: 3.72
	HSE06: 6.53	HSE06: 5.19
axial young's modulus (N/m)	315	152
energy density (kJ/g)	4.41 ($CN_2 \rightarrow$ graphene + N_2)	0.17 ($SiN_2 \rightarrow Si_3N_4 + N_2$)

Table 1. Penta-SiN_2 is thermally and dynamically stable with a band gap of 5.19 eV at HSE06 level, smaller than that of CN_2. More importantly, the symmetry protected double degeneracy along the first Brillouin zone edges still remain in penta-SiN_2 when the spin−orbit coupling is considered in its band structure calculations. The computational procedures and discussions are presented in the Supporting Information.

CONCLUSIONS

In summary, we propose a nitrogen-rich nanosheet, penta-CN_2, which has the Cairo-pentagon-like penta-graphene structure. This structure is beyond any of the previously studied 2D graphitic carbon nitride structures. Our first-principles calculations suggest that penta-CN_2 is dynamically, mechanically, and thermally stable. Systematic study of its vibrational, mechanical, and electronic properties exhibits several hallmarks: (1) The highly puckered structure enables penta-CN_2 to retain a large amount of nitrogen and stay robust against dissociation at room temperature. Moreover, the emerging singly bonded N−N units enable penta-CN_2 to serve as a potential HEDM. (2) Penta-CN_2 has remarkably high in-plane stiffness. The axial Young's modulus is close to that of graphene, and is higher than that of monolayer *h*-BN. (3) The electronic band structures of penta-CN_2 and penta-SiN_2 show an interesting double degeneracy along the first Brillouin zone edges, which is topologically protected by the nonsymmorphic symmetry of the structure, and can be described by a simple tight-binding model. We believe that these findings will enrich the family of nitrogen-rich light element-based materials and stimulate further theoretical and experimental efforts in this field.

ASSOCIATED CONTENT

Supporting Information

The Supporting Information is available free of charge on the ACS Publications website at DOI: 10.1021/acs.jpcc.5b12510.

Zone center vibrational modes of penta-CN_2 and their mode symmetry and Raman and infrared activity, band structure of penta-CN_2 calculated by using the HSE06 functional, bilayer stacking of penta-CN_2, and structural, vibrational, and electronic properties of penta-SiN_2 (PDF)

AUTHOR INFORMATION

Corresponding Author

*(Q.W.) E-mail: qianwang2@pku.edu.cn.

Notes

The authors declare no competing financial interest.

ACKNOWLEDGMENTS

This work is partially supported by grants from the National Natural Science Foundation of China (NSFC-51471004 and NSFC-11174014), the National Grand Fundamental Research 973 Program of China (Grant 2012CB921404), and the Doctoral Program of Higher Education of China (20130001110033). P.J. acknowledges support by the U.S. Department of Energy, Office of Basic Energy Sciences, Division of Materials Sciences and Engineering under Award No. DE-FG02-96ER45579.

REFERENCES

(1) Liu, A. Y.; Cohen, M. L. Prediction of New Low Compressibility Solids. *Science* **1989**, *245*, 841−842.
(2) Niu, C.; Lu, Y. Z.; Lieber, C. M. Experimental Realization of the Covalent Solid Carbon Nitride. *Science* **1993**, *261*, 334−337.
(3) Zimmerman, J. L.; Williams, R.; Khabashesku, V. N.; Margrave, J. L. Synthesis of Spherical Carbon Nitride Nanostructures. *Nano Lett.* **2001**, *1*, 731−734.
(4) Teter, D. M.; Hemley, R. J. Low-Compressibility Carbon Nitrides. *Science* **1996**, *271*, 53−55.
(5) Kim, E.; Chen, C.; Köhler, T.; Elstner, M.; Frauenheim, T. Tetragonal Crystalline Carbon Nitrides: Theoretical Predictions. *Phys. Rev. Lett.* **2001**, *86*, 652−655.
(6) Bucknum, M. J.; Hoffmann, R. A Hypothetical Dense 3,4-Connected Carbon Net and Related B_2C and CN_2 Nets Built from 1,4-Cyclohexadienoid Units. *J. Am. Chem. Soc.* **1994**, *116*, 11456−11464.
(7) Li, Q.; Liu, H.; Zhou, D.; Zheng, W.; Wu, Z.; Ma, Y. A Novel Low Compressible and Superhard Carbon Nitride: Body-Centered Tetragonal CN_2. *Phys. Chem. Chem. Phys.* **2012**, *14*, 13081−13087.
(8) Xiang, H.; Huang, B.; Li, Z.; Wei, S.-H.; Yang, J.; Gong, X. Ordered Semiconducting Nitrogen-Graphene Alloys. *Phys. Rev. X* **2012**, *2*, 011003.
(9) Du, A.; Sanvito, S.; Smith, S. C. First-Principles Prediction of Metal-Free Magnetism and Intrinsic Half-Metallicity in Graphitic Carbon Nitride. *Phys. Rev. Lett.* **2012**, *108*, 197207.
(10) Mahmood, J.; et al. Nitrogenated Holey Two-Dimensional Structures. *Nat. Commun.* **2015**, *6*, 6486.
(11) Zhou, J.; Sun, Q.; Wang, Q.; Jena, P. High-Temperature Superconductivity in Heavily N- or B-Doped Graphene. *Phys. Rev. B: Condens. Matter Mater. Phys.* **2015**, *92*, 064505.
(12) Wang, A.; Zhang, X.; Zhao, M. Topological Insulator States in a Honeycomb Lattice of S-Triazines. *Nanoscale* **2014**, *6*, 11157−11162.
(13) Feng, Y.; Yao, X.; Wang, M.; Hu, Z.; Luo, X.; Wang, H.-T.; Zhang, L. The Atomic Structures of Carbon Nitride Sheets for Cathode Oxygen Reduction Catalysis. *J. Chem. Phys.* **2013**, *138*, 164706.
(14) Li, J.; Cao, C.; Hao, J.; Qiu, H.; Xu, Y.; Zhu, H. Self-Assembled One-Dimensional Carbon Nitride Architectures. *Diamond Relat. Mater.* **2006**, *15*, 1593−1600.

DOI: 10.1021/acs.jpcc.5b12510
J. Phys. Chem. C 2016, 120, 3993−3998

(15) Li, X.; Zhang, S.; Wang, Q. Stability and Physical Properties of a Tri-Ring Based Porous g-C_3N_4 Sheet. *Phys. Chem. Chem. Phys.* **2013**, *15*, 7142−7146.
(16) Li, X.; Zhou, J.; Wang, Q.; Kawazoe, Y.; Jena, P. Patterning Graphitic C−N Sheets into a Kagome Lattice for Magnetic Materials. *J. Phys. Chem. Lett.* **2013**, *4*, 259−263.
(17) Du, A.; et al. Hybrid Graphene and Graphitic Carbon Nitride Nanocomposite: Gap Opening, Electron−Hole Puddle, Interfacial Charge Transfer, and Enhanced Visible Light Response. *J. Am. Chem. Soc.* **2012**, *134*, 4393−4397.
(18) Li, Y.; Zhang, S.; Yu, J.; Wang, Q.; Sun, Q.; Jena, P. A New C═C Embedded Porphyrin Sheet with Superior Oxygen Reduction Performance. *Nano Res.* **2015**, *8*, 2901−2912.
(19) Shi, Z.; Kutana, A.; Yakobson, B. I. How Much N-Doping Can Graphene Sustain? *J. Phys. Chem. Lett.* **2015**, *6*, 106−112.
(20) Zhang, S.; Tsuzuki, S.; Ueno, K.; Dokko, K.; Watanabe, M. Upper Limit of Nitrogen Content in Carbon Materials. *Angew. Chem., Int. Ed.* **2015**, *54*, 1302−1306.
(21) Chaban, V. V.; Prezhdo, O. V. Nitrogen−Nitrogen Bonds Undermine Stability of N-Doped Graphene. *J. Am. Chem. Soc.* **2015**, *137*, 11688−94.
(22) Eremets, M. I.; Gavriliuk, A. G.; Trojan, I. A.; Dzivenko, D. A.; Boehler, R. Single-Bonded Cubic Form of Nitrogen. *Nat. Mater.* **2004**, *3*, 558−563.
(23) Abou-Rachid, H.; Hu, A.; Timoshevskii, V.; Song, Y.; Lussier, L.-S. Nanoscale High Energetic Materials: A Polymeric Nitrogen Chain N_8 Confined inside a Carbon Nanotube. *Phys. Rev. Lett.* **2008**, *100*, 196401.
(24) Timoshevskii, V.; Ji, W.; Abou-Rachid, H.; Lussier, L.-S.; Guo, H. Polymeric Nitrogen in a Graphene Matrix: An *Ab Initio* Study. *Phys. Rev. B: Condens. Matter Mater. Phys.* **2009**, *80*, 115409.
(25) Schmidt, C. L.; Dinnebier, R.; Wedig, U.; Jansen, M. Crystal Structure and Chemical Bonding of the High-Temperature Phase of AgN_3. *Inorg. Chem.* **2007**, *46*, 907−916.
(26) Liu, X.; George, J.; Maintz, S.; Dronskowski, R. B-Cun_3: The Overlooked Ground-State Polymorph of Copper Azide with Heterographene-Like Layers. *Angew. Chem., Int. Ed.* **2015**, *54*, 1954−1959.
(27) Zhang, S.; Zhou, J.; Wang, Q.; Chen, X.; Kawazoe, Y.; Jena, P. Penta-Graphene: A New Carbon Allotrope. *Proc. Natl. Acad. Sci. U. S. A.* **2015**, *112*, 2372−2377.
(28) Lopez-Bezanilla, A.; Littlewood, P. B. σ-π Band Inversion in a Novel Two-Dimensional Material. *J. Phys. Chem. C* **2015**, *119*, 19469−19474.
(29) Li, F.; Tu, K.; Zhang, H.; Chen, Z. Flexible Structural and Electronic Properties of Pentagonal B_2C Monolayer Via External Strain: A Computational Investigation. *Phys. Chem. Chem. Phys.* **2015**, *17*, 24151−6.
(30) Chen, J.; Schusteritsch, G.; Pickard, C. J.; Salzmann, C. G.; Michaelides, A. Two Dimensional Ice from First Principles: Structures and Phase Transitions. *Phys. Rev. Lett.* **2016**, *116*, 025501.
(31) Kresse, G.; Furthmüller, J. Efficient Iterative Schemes for Ab Initio Total-Energy Calculations Using a Plane-Wave Basis Set. *Phys. Rev. B: Condens. Matter Mater. Phys.* **1996**, *54*, 11169−11186.
(32) Blöchl, P. E. Projector Augmented-Wave Method. *Phys. Rev. B: Condens. Matter Mater. Phys.* **1994**, *50*, 17953−17979.
(33) Perdew, J. P.; Burke, K.; Ernzerhof, M. Generalized Gradient Approximation Made Simple. *Phys. Rev. Lett.* **1996**, *77*, 3865−3868.
(34) Heyd, J.; Scuseria, G. E.; Ernzerhof, M. Hybrid Functionals Based on a Screened Coulomb Potential. *J. Chem. Phys.* **2003**, *118*, 8207−8215.
(35) Heyd, J.; Scuseria, G. E.; Ernzerhof, M. Erratum: "Hybrid Functionals Based on a Screened Coulomb Potential" [J. Chem. Phys. 118, 8207 (2003)]. *J. Chem. Phys.* **2006**, *124*, 219906.
(36) Monkhorst, H. J.; Pack, J. D. Special Points for Brillouin-Zone Integrations. *Phys. Rev. B* **1976**, *13*, 5188−5192.
(37) Baroni, S.; de Gironcoli, S.; Dal Corso, A.; Giannozzi, P. Phonons and Related Crystal Properties from Density-Functional Perturbation Theory. *Rev. Mod. Phys.* **2001**, *73*, 515−562.
(38) Giannozzi, P.; et al. Quantum Espresso: A Modular and Open-Source Software Project for Quantum Simulations of Materials. *J. Phys.: Condens. Matter* **2009**, *21*, 395502.
(39) Troullier, N.; Martins, J. L. Efficient Pseudopotentials for Plane-Wave Calculations. *Phys. Rev. B: Condens. Matter Mater. Phys.* **1991**, *43*, 1993−2006.
(40) Lazzeri, M.; Mauri, F. First-Principles Calculation of Vibrational Raman Spectra in Large Systems: Signature of Small Rings in Crystalline SiO_2. *Phys. Rev. Lett.* **2003**, *90*, 036401.
(41) Zhu, Z.; Tománek, D. Semiconducting Layered Blue Phosphorus: A Computational Study. *Phys. Rev. Lett.* **2014**, *112*, 176802.
(42) Tang, W.; Sanville, E.; Henkelman, G. A Grid-Based Bader Analysis Algorithm without Lattice Bias. *J. Phys.: Condens. Matter* **2009**, *21*, 084204.
(43) Ding, K.-W.; Li, X.-W.; Xu, H.-G.; Li, T.-Q.; Ge, Z.-X.; Wang, Q.; Zheng, W.-J. Experimental Observation of TiN_{12}^+ Cluster and Theoretical Investigation of Its Stable and Metastable Isomers. *Chem. Sci.* **2015**, *6*, 4723−4729.
(44) Eremets, M. I.; Hemley, R. J.; Mao, H.-k.; Gregoryanz, E. Semiconducting Non-Molecular Nitrogen up to 240Gpa and Its Low-Pressure Stability. *Nature* **2001**, *411*, 170−174.
(45) Zhang, Z.; Liu, X.; Yakobson, B. I.; Guo, W. Two-Dimensional Tetragonal Tic Monolayer Sheet and Nanoribbons. *J. Am. Chem. Soc.* **2012**, *134*, 19326−19329.
(46) Li, Y.; Hao, J.; Liu, H.; Lu, S.; Tse, J. S. High-Energy Density and Superhard Nitrogen-Rich B-N Compounds. *Phys. Rev. Lett.* **2015**, *115*, 105502.
(47) Talapaneni, S. N.; Mane, G. P.; Mano, A.; Anand, C.; Dhawale, D. S.; Mori, T.; Vinu, A. Synthesis of Nitrogen-Rich Mesoporous Carbon Nitride with Tunable Pores, Band Gaps and Nitrogen Content from a Single Aminoguanidine Precursor. *ChemSusChem* **2012**, *5*, 700−708.
(48) Lee, C.; Wei, X.; Kysar, J. W.; Hone, J. Measurement of the Elastic Properties and Intrinsic Strength of Monolayer Graphene. *Science* **2008**, *321*, 385−388.
(49) Kudin, K. N.; Scuseria, G. E.; Yakobson, B. I. C_2F, BN, and C Nanoshell Elasticity from Ab Initio Computations. *Phys. Rev. B: Condens. Matter Mater. Phys.* **2001**, *64*, 235406.
(50) Levitin, V. *Interatomic Bonding in Solids: Fundamentals, Simulation, and Applications*; Wiley-VCH: 2013.
(51) Young, S. M.; Kane, C. L. Dirac Semimetals in Two Dimensions. *Phys. Rev. Lett.* **2015**, *115*, 126803.
(52) Grimme, S. Semiempirical GGA-Type Density Functional Constructed with a Long-Range Dispersion Correction. *J. Comput. Chem.* **2006**, *27*, 1787−1799.

DOI: 10.1021/acs.jpcc.5b12510
J. Phys. Chem. C 2016, 120, 3993−3998

Supporting Information for

Beyond Graphitic Carbon Nitride: Nitrogen-Rich Penta-CN_2 Sheet

Shunhong Zhang[1], Jian Zhou[2], Qian Wang*[, 1, 2], and Puru Jena[2]

[1] Center for Applied Physics and Technology (CAPT), Key Laboratory of High Energy Density Physics Simulation, Peking University, Beijing 100871, China

[2] Department of Physics, Virginia Commonwealth University, Richmond, VA 23284, USA.

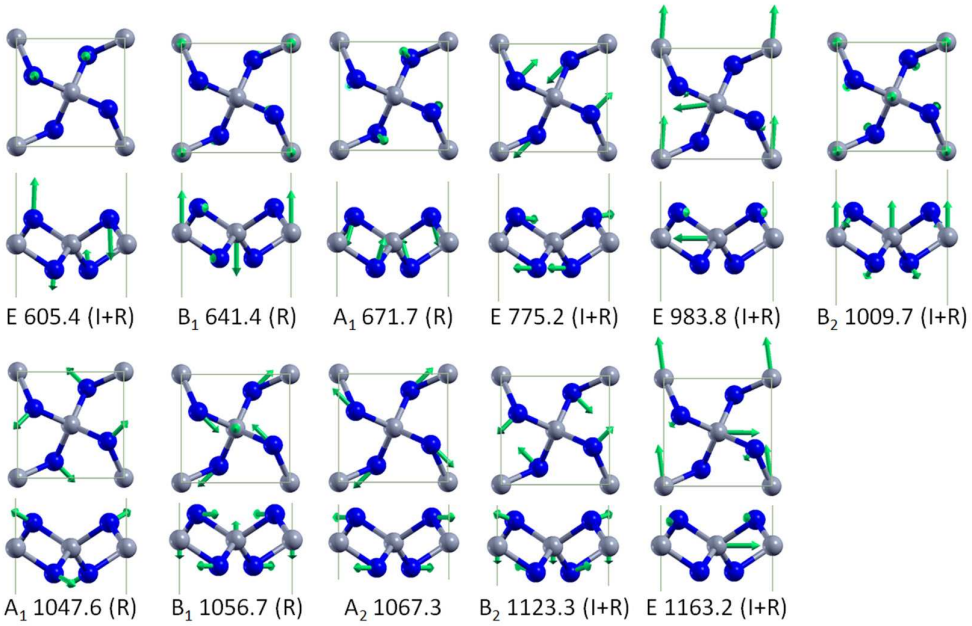

Figure S1 Zone center vibrational modes of penta-CN_2. Grey and blue spheres represent C and N atoms, respectively. Only the non-equivalent modes are shown. Green arrows indicate the vibrational direction, with the length proportional to the amplitude. The mode symmetry, frequency (in cm^{-1}) as well as the Infrared and Raman activity are denoted below the snapshot of each vibrational mode.

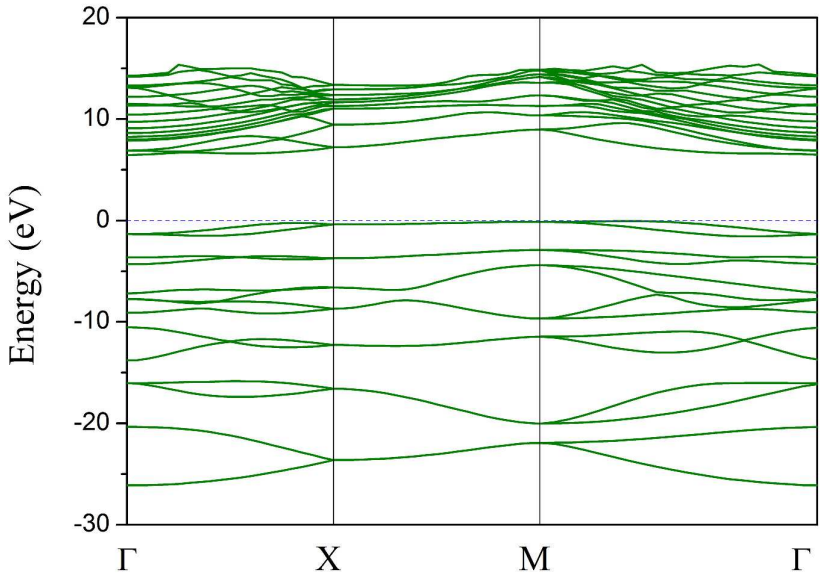

Figure S2 Electronic band structure of penta-CN_2 calculated by using the hybrid HSE06 density functional.

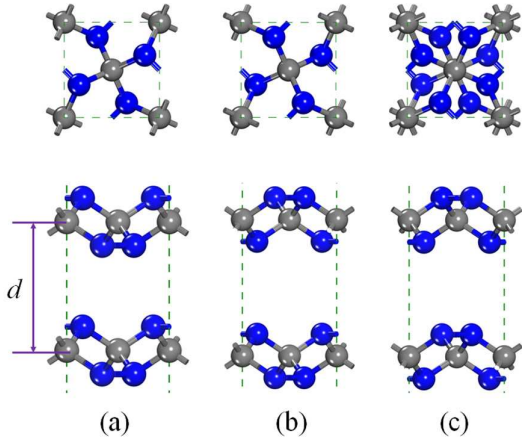

Figure S3 Typical stacking patterns of bilayer penta-CN_2 from top and side views.

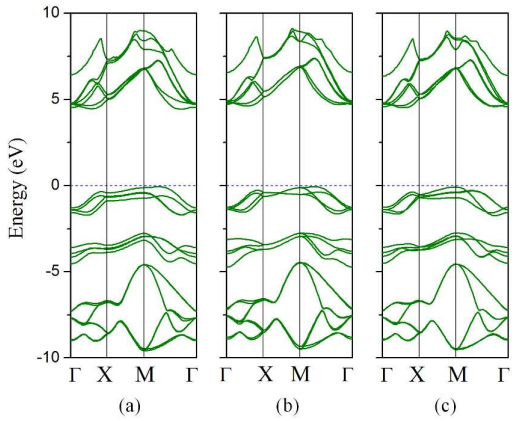

Figure S4 Electronic band structure of bilayer penta-CN_2 corresponding to the stacking patterns presented in Figure S3 (calculated using the PBE functional).

Besides carbon nitride, nanostructured silicon nitride is also a family of extensively studied nitride materials[1-2]. As an extension of penta-CN_2, we tentatively replace all C atoms with Si to build a silicon nitride sheet, penta-SiN_2 (Figure S5a), and fully relax it. The main results regarding penta-CN_2 and penta-SiN_2 are summarized in Table 1 for comparison. The lattice of penta-SiN_2 expands to 4.04 Å due to the longer Si-N bond (1.74 Å). However, the N-N bonds are still single bonds and the bond lengths (1.47 Å) remain almost invariant compared to that in penta-CN_2. Bader's charge analysis shows that silicon atoms transfer ~1.5 electrons (Table 1 in the main text) to each nitrogen atom, much more than the charge transferred in penta-CN_2. Such enhanced ionic character of covalent bonds is due to the larger electronegativity difference between N and Si. The strength of Si-N bond (bond dissociation energy at room temperature: 439 kJ/mol) is known to be weaker than that of C-N bond (bond dissociation energy at room temperature: 770 kJ/mol)[3]. As a consequence, the in-plane stiffness is significantly impaired: the axial Young's modulus is only about half of that of penta-CN_2 (Table 1).

Our calculated phonon spectrum shows that penta-SiN_2 is also dynamically stable (Figure

S5b). AIMD simulations further confirm its room temperature thermal stability (Figure S6). More importantly, penta-SiN_2 has negative formation energy of -0.14 eV/atom (with reference to diamond Si and N_2 molecule), implying that it is likely to realize such a compound using diamond Si and gaseous nitrogen as reactants. For its future characterization Raman and infrared spectra are also calculated and presented in Figure S5b. If we take β-Si_3N_4 and N_2 as references, the formation energy of penta-SiN_2 becomes positive, indicating that penta-SiN_2 can also release energy when decomposing into these two compounds. However, the energy density of penta-CN_2 is only 0.17 kJ/g. Two reasons are responsible for this low energy density: the atomic mass of Si is larger than C, decreasing the weight percentage of N; some N contents are stored in β-Si_3N_4 in the reaction $3SiN_2 \rightarrow Si_3N_4+N_2$, rather than forming triply bonded N_2 molecules. The electronic energy band dispersions and band compositions of penta-SiN_2 (Figure S5c) resemble that of penta-CN_2, however, the band gap is smaller (3.72 eV obtained by PBE functional and 5.19 eV predicted by HSE06 functional, see Figure S7). Notably, the symmetry protected double degeneracy along the first Brillouin zone edges retains in penta-SiN_2. Band structure calculation including spin-orbital coupling doesn't change such band degeneracy character.

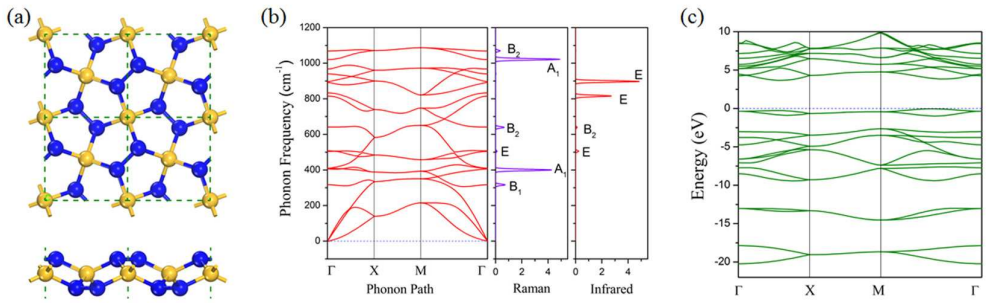

Figure S5 (a) Optimized structure of penta-SiN_2. Yellow and blue spheres are Si and N atoms, respectively. (b) The corresponding phonon spectra, as well as the Raman and infrared intensity (in arbitrary unit) of the zone center modes. (c) The electronic band structure (GGA/PBE functional) of penta-SiN_2.

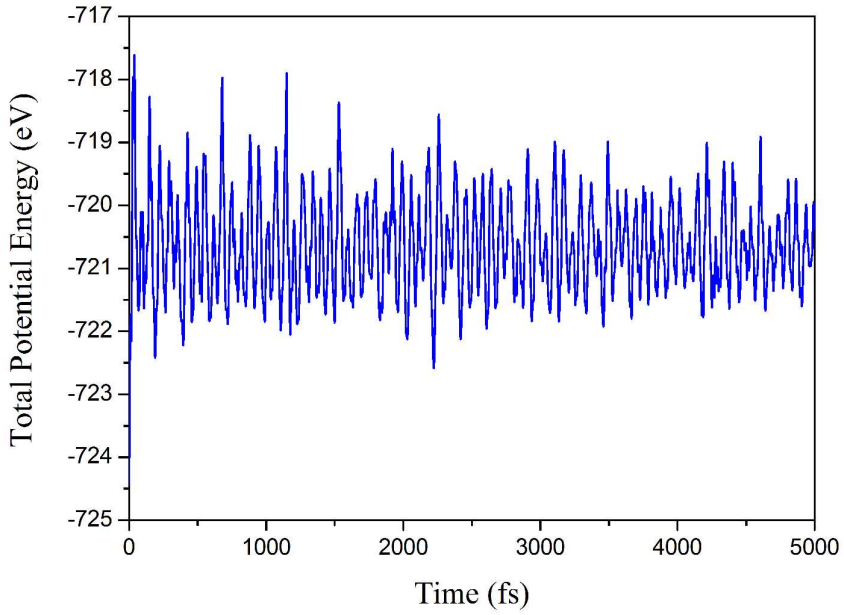

Figure S6 Fluctuation of potential energy of penta-SiN_2 (4×4 supercell) during a NVT AIMD simulation at 300 K.

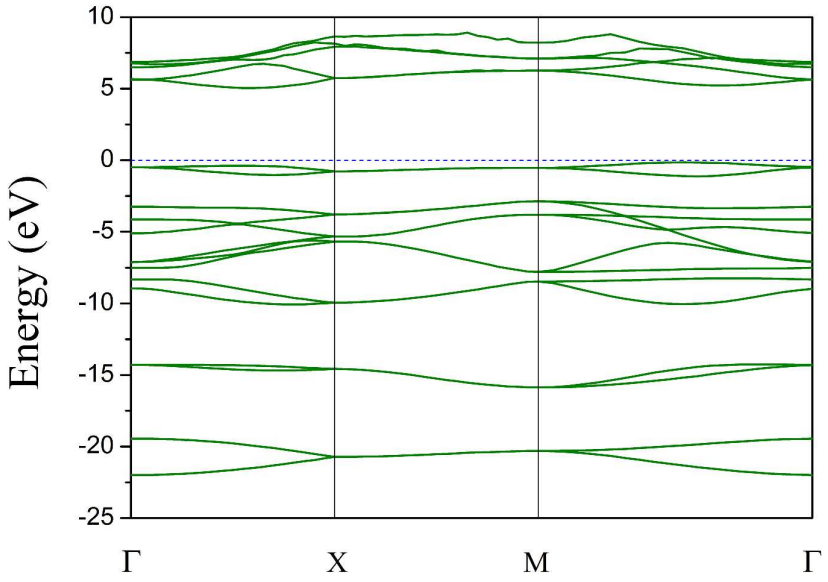

Figure S7 Electronic band structure of penta-SiN_2 calculated by using the hybrid HSE06 density functional.

References

1. Guo, Y.; Zhang, S.; Wang, Q., Electronic and Optical Properties of Silicon Based Porous Sheets. *Phys. Chem. Chem. Phys.* **2014**, *16*, 16832-16836.

2. Ding, Y.; Wang, Y., Density Functional Theory Study of the Silicene-Like Six and Xsi_3 (X = B, C, N, Al, P) Honeycomb Lattices: The Various Buckled Structures and Versatile Electronic Properties. *J. Phys. Chem. C.* **2013**, *117*, 18266-18278.

3. Dean, J. A., *Lange's Handbook of Chemistry*, 15 ed.; McGraw-Hill: New York, 1999.